Available online at www.sciencedirect.com
ScienceDirect
Polymer 47 (2006) 6797–6807
polymer
www.elsevier.com/locate/polymer

Relationship between structure and dynamic mechanical properties of a carbon nanofiber reinforced elastomeric nanocomposite

Antonis Kelarakis, Kyunghwan Yoon, Rajesh Somani, Igors Sics, Xuming Chen, Benjamin S. Hsiao*, Benjamin Chu*

Department of Chemistry, Stony Brook University, Stony Brook, NY 11794-3400, USA

Received 11 May 2006; received in revised form 28 June 2006; accepted 28 June 2006
Available online 14 August 2006

Abstract

The tensile and dynamic mechanical properties of a nanocomposite, containing modified carbon nanofibers (MCNFs) homogenously dispersed in an elastomeric ethylene/propylene (EP) copolymer semicrystalline matrix (84.3 wt% P), have been correlated with the structure development. These properties were characterized by in situ synchrotron X-ray diffraction during stretching, dynamic mechanical analysis and X-ray analysis techniques over a wide temperature range. Upon sequential drawing, the tensile strength of the nanocomposite film was notably higher than that of the unfilled polymer even though both samples exhibited a similar amount of crystal fraction and the same degree of crystal orientation, revealing the effect of nanofiller reinforcement in the semicrystalline matrix. The mechanical spectra of the 10 wt% MCNF filled samples in both stretched and non-stretched states showed broadening of the elastic modulus at high temperatures, where the corresponding crystallinity index also decreased. It is conceivable that a significant fraction of chain orientation is induced in the vicinity of the nanofillers during stretching, and these stretched chains with reduced mobility significantly enhance the thermal mechanical properties.

Keywords: Carbon nanofiber; EP copolymer; Nanocomposite

1. Introduction

Since their introduction [1] by Iijima in 1991, carbon nanotubes and carbon nanofibers (CNT and CNF, respectively) have become a subject of intensive research in the polymer community. It is now well established that polymer nanocomposites based on CNT and CNF can exhibit superior mechanical properties [2,3], high electrical conductivity [4] and advanced thermo-mechanical properties [4]. In particular, the incorporation of CNTs and CNFs in thermoplastic polymers by conventional melt mixing appears to be a practical way for development of a new class of filled materials with unique properties [5].

The major challenges in the preparation of nanocomposites containing CNT or CNF are two: (1) the manipulation of filler orientation and (2) the control of filler dispersion. The subject of nanofiller orientation has been addressed in several studies. For example, without polymer, the alignment of CNTs can be achieved by using chemical vapor deposition (CVD) methods [6–8]. The post growth alignment techniques using selective laser ablation [9], external forces such as microfluidic [10], air flow [11], electric [12] and magnetic [13] fields have also been reported. In the presence of polymer, a variety of techniques have been demonstrated to promote the alignment of nanofillers such as shearing of nanocomposite thin film (through microtoming) [14], drawing a nanofiller suspension (through a micropore filter) [15], electrospinning [16,17] and mechanical stretching [18,19]. Homogenous dispersion of nanofillers in the polymer matrix can be achieved by the development of strong van der Walls bonding between nanofillers and polymers. In order to overcome the inherent

* Corresponding authors. Tel.: +631 632 7793 (B.S.H.), +631 632 7928 (B.C.); fax: +631 632 6518.
E-mail addresses: bhsiao@notes.cc.sunysb.edu (B.S. Hsiao), bchu@notes.cc.sunysb.edu (B. Chu).

0032-3861/$ - see front matter © 2006 Elsevier Ltd. All rights reserved.
doi:10.1016/j.polymer.2006.06.070

incompatibility between nanofillers and the polymer matrices, as well as to minimize the strong tendency of filler self-assembly, chemical treatment of the nanofiller surface is often necessary. It has been demonstrated that covalent attachment of functional groups on the graphitic sidewalls of CNTs and CNFs can promote their dispersion into the polymeric matrices [20–23], thus, ensuring significant energy and load transfer across the nanofiller–matrix interface and enhancing the mechanical performance of nanocomposites.

In this study, the chosen filler system was the CNF functionalized by grafting of polypropylene to its sidewalls; the matrix was ethylene/propylene (E/P) random copolymer having dominant P content (84.3 wt%). The homogenous distribution of the modified-CNF (MCNF) in the EP matrix has been confirmed in our previous studies [24]. We selected CNF rather than CNT because surface of the former is easier to modify – the CNF surface has a significant fraction of layer edge defects due to the presence of tilted graphite layers with respect to the CNF axis [25]. The choice of the EP copolymer was based on the combined elastomeric and thermoplastic nature of the material, which gives rise to interesting tensile properties [26,27]. This thermoplastic elastomer consists of hard segments based on isotactic polypropylene (iPP) crystals and soft segments dominated by the amorphous EP copolymer chains. The iPP crystals act as physical cross-links leading to high strength at room temperature, but they can be melted enabling the easy processing of this material. It is thought that the presence of a CNF scaffold can provide another level of the network structure to enhance some mechanical properties.

Despite the considerable body of work reported on the mechanical reinforcement of elastomers [28,29] and polypropylene materials [17,30–32] with incorporation of CNTs and CNFs, the relationships between the deformation mechanism and the polymer chain dynamics of these filled materials based on the semicrystalline matrix are still not clear. The deformation mechanism of the chosen nanocomposite system has been the subject of a recent report by us [24]. The WAXD data were obtained in situ during stretching at room temperature and were analyzed with respect to the stress–strain curves of both filled and unfilled samples. Results indicated that the polymer matrix in the nanocomposite appeared to experience a reduced stress compared with the pure polymer, which can be attributed to the efficient load transfer from the polymer matrix to the MCNF. However, as the crystalline morphology (crystallinity and crystal orientation) of the filled and unfilled polymers was not the same at room temperature, such a comparison might not be meaningful.

In this study, the stretching was carried out at a higher temperature (e.g. 40 °C), where both crystal fraction and crystal orientation in the resulting filled and unfilled samples can be adjusted to similar levels. With such ''stretched samples'', we have investigated the polymer chain dynamics in the vicinity of MCNF where the chains exhibited non-bulk characteristics. To achieve our goal, the combined tensile stretching and dynamic mechanical analysis techniques together with synchrotron X-ray diffraction were used. The dynamics of polymer chains in the nanocomposite was examined by considering (1) the effect of sequential drawing with respect to the orientation of the nanofillers and the polymer crystals; (2) the mechanical spectra of the filled and unfilled samples in both stretched and unstretched states; and (3) the structure (i.e., crystallinity and orientation) and mechanical property relationships over a wide temperature range, e.g. from room temperature up to complete melting.

2. Experimental

2.1. Materials and preparation

The EP random copolymer was provided by ExxonMobil Chemical Company and is an experimental sample similar to one of the commercial ''Vistamaxx'' specialty elastomers [26]. The copolymer was synthesized with the aid of discrete metallocene catalyst and had 84.3 wt% propylene content, $M_n = 9.6 \times 10^4$ g/mol and $M_w = 1.7 \times 10^5$ g/mol. Carbon nanofibers were provided by Applied Sciences with the trade name of Pyrograf III, PR-24-HHT. The diameter of CNF varied from 60 to 150 nm and the length was between 30,000 and 100,000 nm. No further purification on the CNF was performed.

The chemical schemes for the modification of CNF by grafting short polypropylene chains on the graphitic sidewalls have previously been reported in detail [33,34]. In brief, a polypropylene-*graft*-maleic anhydride polymer purchased from Aldrich ($M_w = 9100$ g/mol, $M_n = 3900$ g/mol, acid number = 47 mg KOH/g) was used as the grafting polymer. CNF was first oxidized by a sulfuric/nitric acid mixture and then reduced with sodium borohydride in absolute ethanol. The resulting CNF sample and polypropylene-*graft*-maleic anhydride polymer were dispersed in 1,2-dichlorobenzene and the mixture was heated under stirring. The dispersion was filtered in hot conditions and washed with warm 1,2-dichlorobenzene. The filtered solid was placed in a soxhlet extraction apparatus (until constant weight) to ensure the complete removal of unattached polymer. The recovered polypropylene-grafted CNF sample was then dispersed in xylene by ultrasonication and the EP copolymer was added in the hot dispersion. The mixture was precipitated into cold methanol, filtered, and dried in vacuum for a day. For comparison purposes, the identical treatment was also applied for the pure EP copolymer. Based on SEM examinations, CNFs were homogenously dispersed in the EP matrix.

2.2. Instrumentation and experimental procedures

In situ time-resolved wide-angle X-ray diffraction (WAXD) experiments were performed at the X27C beamline in the National Synchrotron Light Source (NSLS), Brookhaven National Laboratory (BNL), USA. The wavelength of the synchrotron radiation was 0.1371 nm. Two-dimensional WAXD patterns were collected using a MAR CCD (MARUSA, Inc.), X-ray detector with a resolution of 1024 × 1024 pixels (pixel size = 158.44 μm). The acquisition time for each image

was 30 s. The sample-to-detector distance was 111.7 mm. The diffraction angle was calibrated by using an Al_2O_3 standard.

Uniaxial stretching of polymer/nanocomposite samples was accomplished by using a modified Instron 4442 tensile apparatus equipped with a temperature chamber. This tensile apparatus allowed symmetric deformation of the sample at a constant rate (the chosen rate was 10 mm/min in this study) and the detection area on the sample remained constant in space. The tensile samples were prepared by press molding of polymer/nanocomposite granules at 150 °C under a pressure of 4000 kg/m^2 for 3 min. The molded samples were quenched by ice water. The samples were cut into dumbbell shape with a length of 25 mm. The strain at time t was calculated as $(l - l_0)/l_0$, where l is the length of the sample at time t and l_0 is the original length of the sample.

A dynamic mechanical analyzer (Rheometric Scientific, model RSA II) was used to measure the tensile modulus of the unfilled and the 10 wt% filled samples. The measurements were carried out in a tensile mode, at the heating rate of 2 °C/min, from room temperature to 80 °C, at a fixed frequency of 10 rad/s (within the linear region of viscoelasticity). The samples were cut in rectangular strips.

2.3. WAXD data analysis

Two-dimensional (2D) WAXD patterns were corrected for incident beam fluctuations, and the air and instrument background scattering was subtracted from all measured patterns. In order to convert the 2D flat-plate WAXD image into an undistorted geometry in reciprocal space, the ''Fraser'' correction procedure was adopted [35]. In addition, the ''halo method'' [36] was used to estimate the oriented and unoriented fractions of polymer phases in the nanocomposite. The basic assumption of the ''halo method'' is that the azimuthally independent component of the total scattered intensity is directly proportional to the unoriented portion of the sample. For each azimuthal scan, the minimum value of the intensity is considered as the intensity that arises from the unoriented scatterers. The isotropic contribution thus obtained can be subtracted from the 2D WAXD pattern, yielding the contribution of the oriented scatterers.

Deconvolution of spherically integrated WAXD intensity profiles (Fraser corrected) into the amorphous and crystalline phases was carried out by the Peak Fit program. The shape of the amorphous peak was obtained from the WAXD pattern of the sample in the molten state, which was fitted with three Gaussian functions. Additional Gaussian functions were used to fit the crystalline peaks. This fitting procedure provided the crystallinity index of the sample. The total crystallinity index X_C^T can be estimated by the following equation:

$$X_C^T = 100\% - X_A^T \quad (1)$$

where X_A^T represents the area percentage of the amorphous contribution. The similar peak fit procedures were used to deconvolute the intensity profiles of the oriented and unoriented components of the crystalline phase (denoted as X_C^O and X_C^U, respectively). Azimuthal scans of the diffraction peaks from polymer crystals as well as MCNF were performed on the oriented fraction of the 2D WAXD image. The azimuthal profile was fitted with a Lorentzian function and the area was divided by the corresponding peak height. The integral breadth (IB) thus obtained was considered as a measure of the degree of alignment for both polymer crystals and nanofillers along the stretching direction.

3. Results

3.1. WAXD characterization of undeformed samples

The circularly averaged WAXD intensity profiles for the undeformed unfilled and 10 wt% filled samples obtained at 27 °C (room temperature) and 40 °C are presented in Fig. 1. Also included in this figure are the deconvoluted peaks of these intensity profiles, which can be divided into amorphous and crystalline fractions. At both temperatures, the deconvoluted crystal peaks indicate the coexistence of α-monoclinic [37,38] and γ-triclinic [39–43] forms of iPP crystals. For example, the positions of the discrete reflections shown in Fig. 1 can be indexed as α(110)/γ(111) at $q = 10.2\ nm^{-1}$, α(040)/γ(008) at $q = 11.8\ nm^{-1}$, α(130) at $q = 13.0\ nm^{-1}$, γ(117) at $q = 13.9\ nm^{-1}$ and α(111)/γ(202) at $q = 15.1\ nm^{-1}$ (we note that γ(117) and α(130) reflections do not overlap each other). The presence of γ phase iPP crystals in P dominant random EP copolymers has been reported earlier [43]. It was found that the content of γ phase reached a maximum value at about 15 wt% ethylene [43], which is close to the composition of the chosen EP copolymer.

Several unique features were observed in Fig. 1. (1) The fraction of γ form crystals in the 10 wt% filled sample was lower than that in the unfilled EP copolymer at both room temperature and 40 °C. However, the percentage of total crystallinity index, X_C^T, of the filled samples was slightly higher than that of the unfilled samples. This behavior is consistent with the well known behavior that carbon nanofillers can nucleate crystallization of α-form crystals in iPP [44–46]. (2) The comparison of the intensity profiles at both temperatures indicates that partial melting of polymer crystals took place at 40 °C. (3) The peak at $q = 18.4\ nm^{-1}$ in the WAXD profile of the 10 wt% nanocomposite corresponds to 3.4 Å spacing, which can be attributed to the inter-shell spacing [47–49] within the CNF structure (d_{002}). The Bragg peak that corresponds to d_{002} spacing is referred to as (002) reflection. The term is adopted in this work hereafter.

3.2. In situ WAXD during deformation of unstretched samples

In situ WAXD results during stretching of the chosen nanocomposite at room temperature have been reported by us recently [24]. Here, we present the WAXD data during first stretching of this nanocomposite at 40 °C. The selection of this particular temperature is for the following reason. Drawing of both filled and unfilled samples (up to a strain of 6)

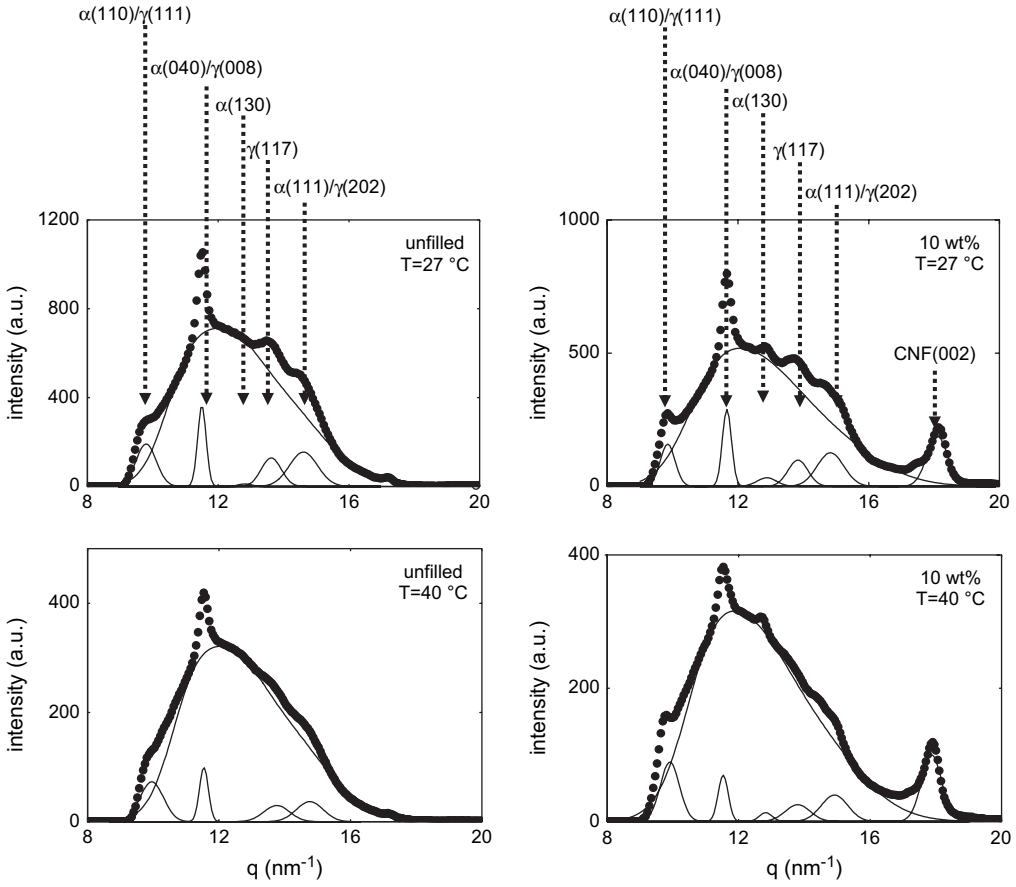

Fig. 1. Deconvolution of the circularly averaged WAXD intensity profiles into amorphous and crystalline components. The WAXD patterns were acquired from the unstretched state of the unfilled and 10 wt% filled samples at room temperature (ca. 27 °C) and 40 °C.

at 40 °C allowed the fabrication of the same level of mass fraction for each crystal phase (i.e., α or γ phase) and a comparable degree of crystal orientation. The comparison of the results from the filled and unfilled polymers thus becomes essential for a meaningful understanding of the effect of nanofillers (i.e. MCNF) on the polymer chain dynamics in nanocomposites. We have also carried out deformation at other temperatures, such as room temperature, 55 and 60 °C. However, the fraction of the γ phase and the degree of crystal orientation in both samples could not be made the same at these temperatures.

The stress–strain curves and selected WAXD patterns acquired during stretching at 40 °C of the unfilled and 10 wt% nanocomposite unstretched samples are shown in Fig. 2. Upon stretching, the WAXD patterns became anisotropic, indicating the development of orientation for both polymer crystals and MCNF along the drawing direction. The circularly averaged WAXD intensity profiles of the highly stretched (strain = 6) samples were compared with those of unstretched samples in Fig. 3. On the basis of the integrated area ratio between the γ(117) and α(130) peaks, it can be concluded that the fraction of the γ phase decreases in favor of the development of the α phase during stretching. In fact, no γ phase was detected at the end of stretching in both samples. The transition of γ to α phase of isotactic polypropylene during stretching has been studied in detail for poorly crystallized polypropylene

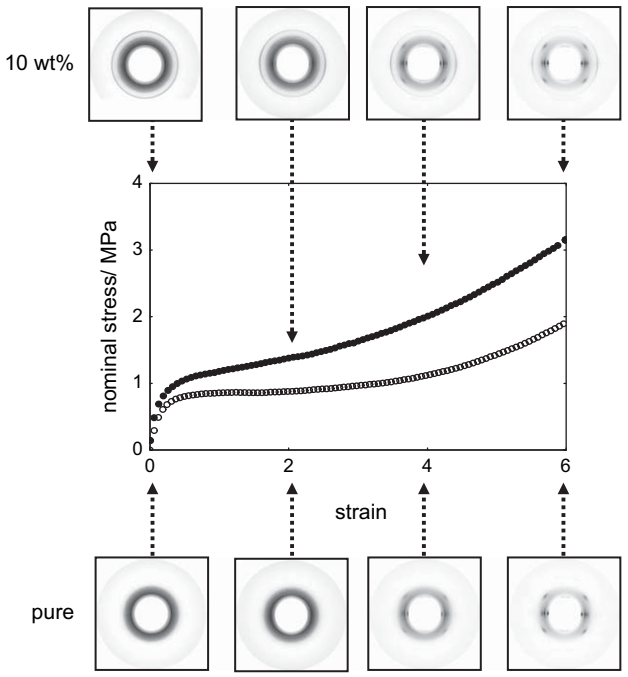

Fig. 2. Stress–strain curves and selected WAXD patterns acquired during the 1st stretching of the unfilled polymer (unfilled circles) and the 10 wt% filled polymer (filled circles) at 40 °C.

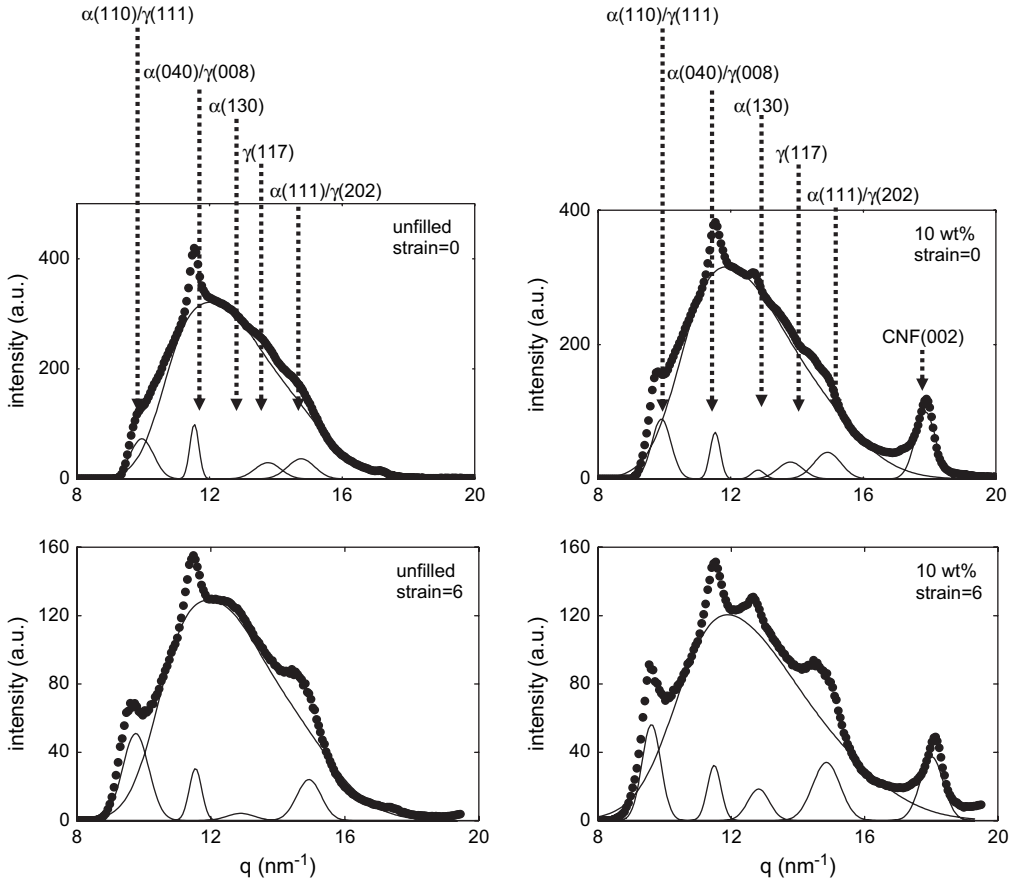

Fig. 3. Deconvolution of the circularly averaged WAXD intensity profiles into amorphous and crystalline components. The WAXD patterns of the pure copolymer and the 10 wt% nanocomposite were acquired during stretching (with strain up to 6) at 40 °C.

materials with elastomeric characteristics [50,51]. This transition has been attributed to the non-parallel chain structure of the γ phase, in contrast with the parallel arrangement of the α phase. In particular, for the α phase, the succession of bilayers is such that the chain axes are parallel; whereas for the γ phase the chain axes tilt 81° of each other. The non-parallel chain configuration in the γ phase does not permit complete alignment along the stretching direction and, therefore, γ phase is preferentially destroyed upon deformation.

The total and unoriented crystallinity indices (X_C^T and X_C^U, respectively) are plotted as a function of strain in Fig. 4 for both filled and unfilled samples. In these samples, the behavior of mechanical induced ''melting'', i.e., the destruction of some crystal phase, was evident at relatively low strains − the value of X_C^T decreased at low strains. Upon further elongation, the X_C^T value was found to increase while X_C^U decreased with strain, which suggests that strain-induced crystallization took place where new oriented crystals were formed (as the oriented crystallinity index increased). At the end of the stretching process, both samples were found to possess about the same values of total crystallinity (X_C^T). The above results, together with the observations of the α and γ phase changes in Fig. 3 suggest that the transformation from γ to α phase is sequential, i.e., the destruction of the γ phase followed by the formation of the α phase, instead of going through a real phase transition.

Fig. 5 illustrates that the integral breadth (IB) of the hybrid crystal peak α(110)/γ(111) at $q = 10.2\ \mathrm{nm}^{-1}$ decreased with strain in both the samples. The IB value in the pure copolymer was generally higher than that in the filled sample. However, at higher strains, the degree of crystal orientation in both filled and unfilled samples became the same, in spite of the fact that

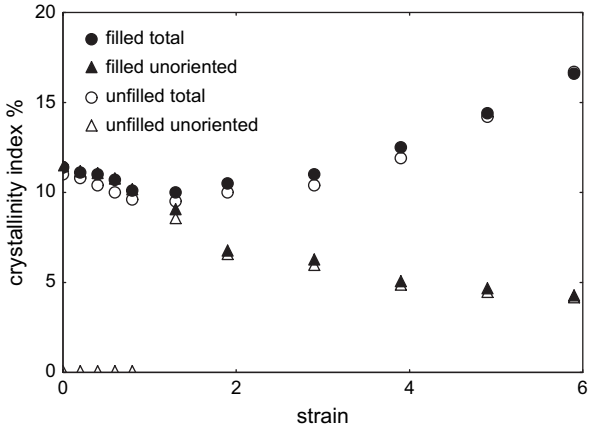

Fig. 4. Total (circles) and unoriented (triangles) crystallinity indices (X_C^T and X_C^U, respectively) as a function of strain determined during extension of the unfilled polymer (unfilled symbols) and 10 wt% filled polymer (filled symbols) at 40 °C.

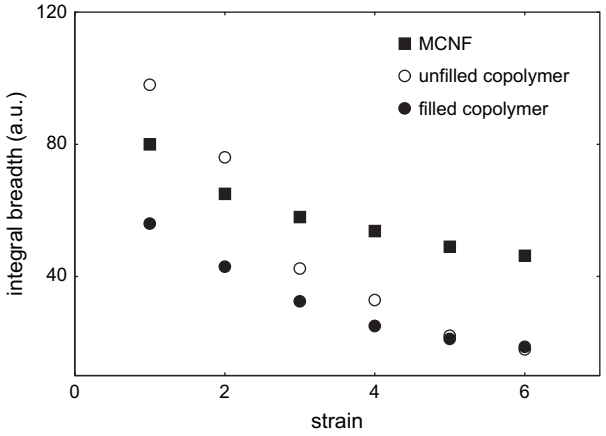

Fig. 5. Integral breadths (IB) corresponding to the hybrid α(110)/γ(111) reflection of the polymer crystals (filled symbols for the filled sample, open symbols for the unfilled sample) and the (002) reflection of MCNFs (squares) obtained during stretching at 40 °C.

considerably higher stress was developed in the nanocomposite. This behavior indicates that the load transfer between the matrix and the MCNF filler is quite efficient and the polymer matrix experiences a reduced effective stress compared to the bulk stress. In Fig. 5, the IB determined from the azimuthal profile of the (002) reflection in MCNF also decreased with strain, suggesting the increase of MCNF filler alignment during stretching. Due to the large stiffness of the MCNF phase, the extent of the nanofillers orientation was consistently lower than the orientation of the polymer crystals.

In order to gain a better understanding on how one can manipulate the orientation of MCNF in the nanocomposite by uniaxial stretching, the samples were also deformed at other temperatures: 27, 55 and 60 °C. The IB values of the MCNF component obtained in all stretching measurements are plotted as a function of strain in Fig. 6a and as a function of stress in Fig. 6b (the data at 55 and 60 °C were obtained up to the maximum strain of 23 and 8, respectively). It was seen that under the same strain, the MCNF phase exhibited a narrower IB value or stronger orientation at lower temperatures as a result of the higher viscosity of the polymer matrix and the higher corresponding stress. On the other hand, under the same stress, MCNF exhibited stronger orientation at higher temperatures. This observation underlines the effect of MCNFs on the mechanical reinforcement of semicrystalline polymers at elevated temperatures, where the role of crystalline structure becomes weak.

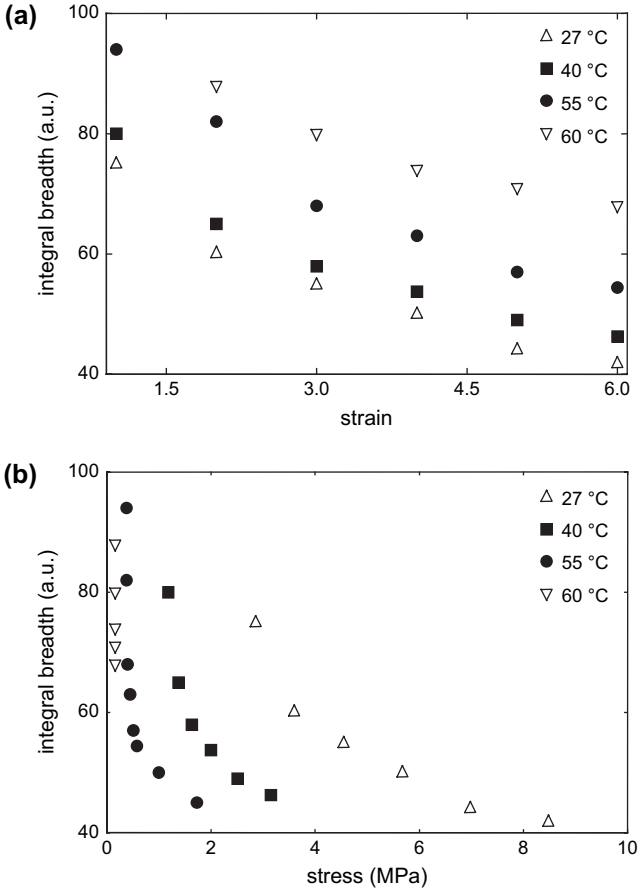

Fig. 6. Integral breadths (IB) corresponding to the (002) reflection of MCNFs (squares) obtained during stretching of the 10 wt% filled polymer at the temperatures indicated. The same data are plotted as a function of (a) strain and (b) stress.

3.3. In situ WAXD during deformation of ''stretched-set'' samples

When the stretched samples were held at a constant strain under tension and cooled down to room temperature, the samples retained certain degrees of polymer crystal and MCNF orientations. These samples can be considered as being a ''permanent set''. For this purpose, a pair of filled and unfilled samples were subjected to stretching with strain up to 6.0 at 40 °C and were cooled down to room temperature while held at a constant strain and annealed for 1 h. The resulting samples were referred to hereafter as the ''stretched-set'' or ''stretched'' samples. The stress–strain curves of the stretched unfilled/filled samples obtained during uniaxial deformation until break at room temperature are illustrated in Fig. 7. The tensile strength of the stretched samples was significantly higher than that of the unstretched samples (during first stretching) at room temperature. The strong intensity distribution of the polymer crystal as well as MCNF reflections (Fig. 7) is indicative of highly oriented structures. In both samples, the amount of unoriented crystals was low in the beginning of deformation and rapidly approached to zero at higher strains. This is seen in Fig. 8, where X_C^T and X_C^U are plotted as a function of strain for both unfilled and filled samples. It is interesting to note the absence of the strain-induced ''melting'' step at low strains (as seen in Fig. 4), which is probably because the stretched samples did not contain a significant fraction of defected crystals that could be destroyed upon stretching.

The extent of orientation of both polymer crystals and the MCNF was found to increase with strain, as shown in Fig. 9. At the same strain, the polymer crystals in the unfilled sample exhibited a degree of orientation slightly higher than

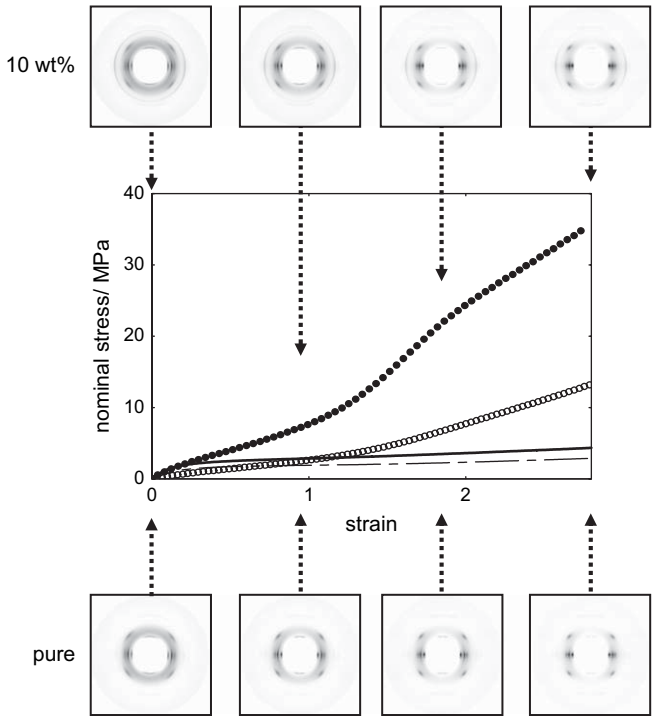

Fig. 7. Stress–strain curves and selected WAXD patterns acquired during 2nd stretching of the unfilled polymer (unfilled circles) and the 10 wt% filled polymer (filled circles) at room temperature. The lines indicate the tensile data obtained during the 1st stretching at room temperature of the unfilled (dashed line) and the 10 wt% filled (solid line) samples.

that in the filled sample, despite the fact that the stress was considerably lower in the unfilled polymer. This is consistent with the notion that the polymer crystals experienced a reduced stress in the filled copolymer due to the presence of MCNF or an effective load transfer from the polymer matrix to MCNF. The large difference in the tensile strength developed between the two systems and the above results indicate a direct correlation between the MCNF alignment and the extent of mechanical reinforcement in the nanocomposites.

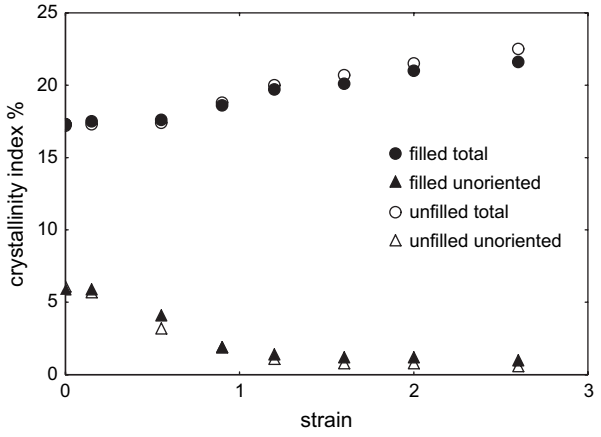

Fig. 8. Total (circles) and unoriented (triangles) crystallinity indices (X_C^T and X_C^U, respectively) as a function of strain determined during 2nd stretching of the unfilled polymer (unfilled symbols) and 10 wt% nanocomposite (filled symbols) at room temperature.

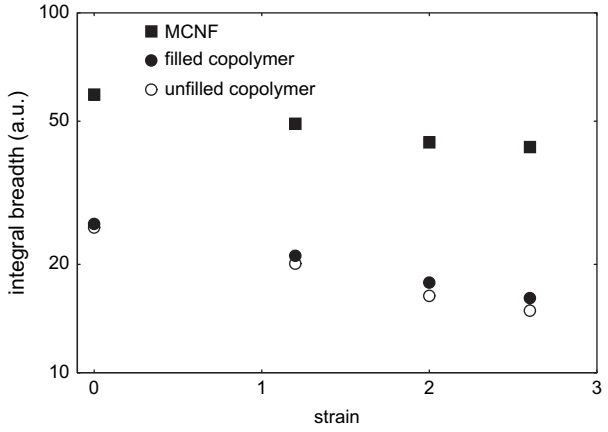

Fig. 9. Integral breadths (IB) corresponding to the hybrid α(110)/γ(111) reflection of the polymer crystals (filled circles for the filled sample, open circles for the unfilled) and the (002) reflection of MCNFs (squares) obtained during 2nd stretching at room temperature.

3.4. Dynamic mechanical properties

The dynamic mechanical spectra of both filled and unfilled samples, obtained at a heating rate of 2 °C/min, are presented in Fig. 10. Selected WAXD patterns were also included in this figure; they were obtained during heating of the samples from room temperature. It was seen that the addition of MCNF resulted in a significant increase (ca. 40%) in the storage modulus E' of the polymer matrix at room temperature and a 300% increase at 75 °C. The dynamic mechanical properties of the stretched samples were also examined and the values of

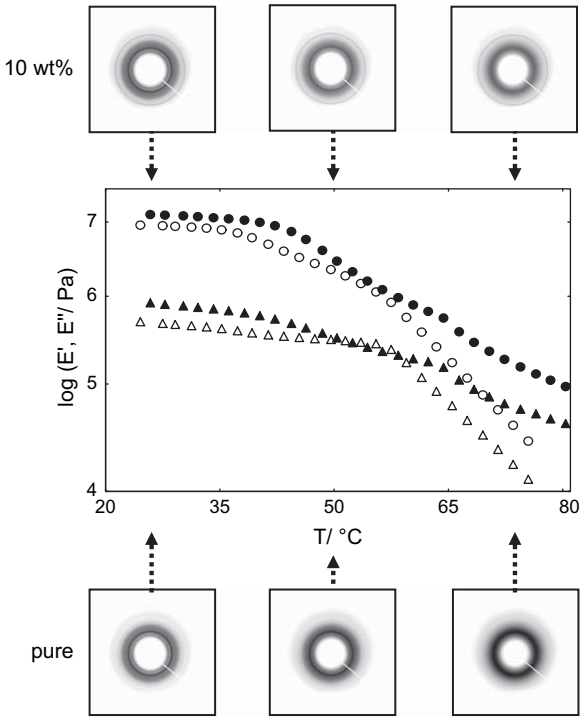

Fig. 10. Temperature dependence of E' (circles) and E'' (triangles) and selected WAXD patterns of the unfilled polymer (open symbols) and the 10 wt% filled polymer (filled symbols) in the unstretched state.

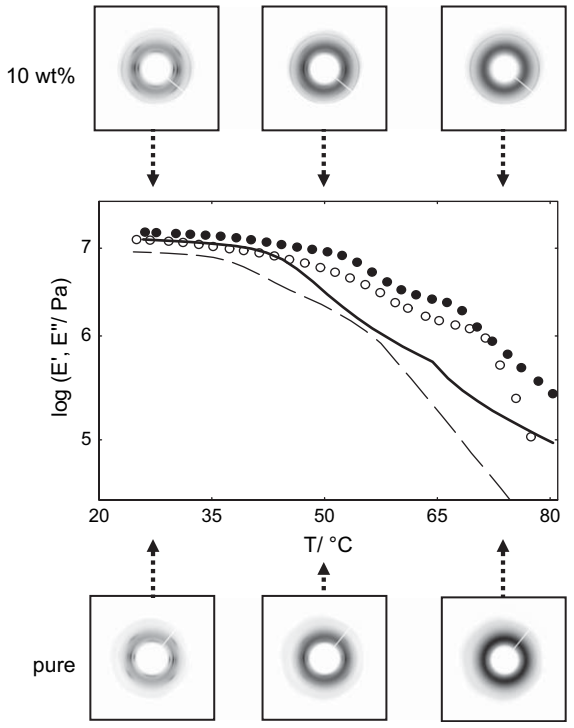

Fig. 11. Temperature dependence of E' (circles) and selected WAXD patterns of the unfilled polymer (open symbols) and the 10 wt% filled polymer (filled symbols) in the stretched state. The lines represent the E' data obtained from these samples in the unstretched state (dashed line for the unfilled polymer, thick line for the filled polymer) adopted from Fig. 10.

storage modulus E' for all four samples are illustrated in Fig. 11. It is apparent that the stretched samples, both filled and unfilled, exhibited superior mechanical performance in comparison with the corresponding unstretched samples.

The overall enhancement of the dynamic mechanical response by MCNF in stretched and unstretched states is illustrated in Fig. 12, where the tan δ values for the four samples are plotted as a function of temperature. It was seen that upon heating, the tan δ value gradually deviated from the baseline established at low temperatures. Among the four samples,

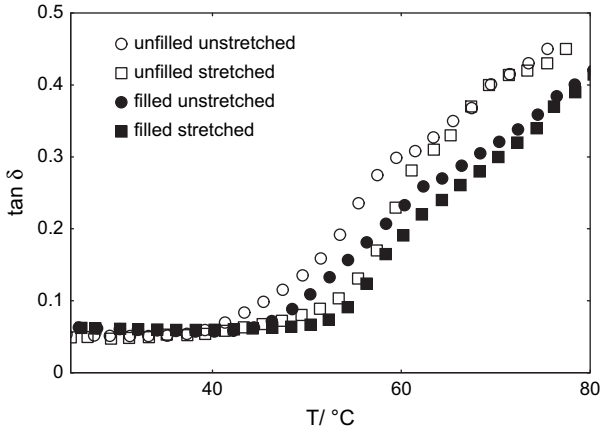

Fig. 12. Temperature dependence of tan δ of the samples: unstretched unfilled (unfilled circles), stretched unfilled (unfilled squares), 10 wt% unstretched filled (filled circles), stretched filled (filled squares) samples.

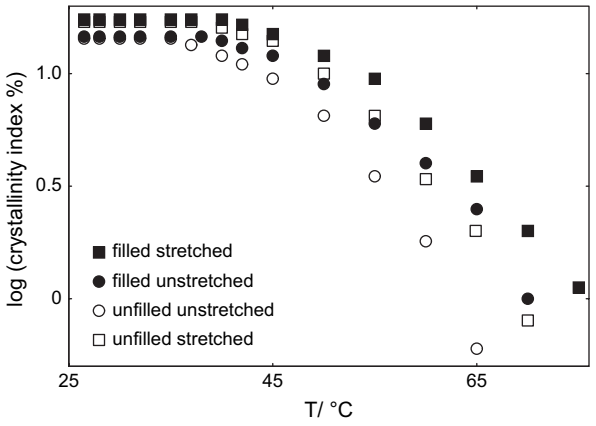

Fig. 13. Temperature dependence of the total crystallinity indices of the samples: unstretched unfilled (unfilled circles), stretched unfilled (unfilled squares) 10 wt% unstretched filled (filled circles), stretched filled (filled squares) samples.

the temperature at which the deviation occurred exhibited the lowest value for the unstretched unfilled sample (~37 °C), followed by the stretched unfilled sample (~40 °C), the unstretched filled sample (~42 °C), and the stretched filled sample (~44 °C).

The crystallinity indices for the four samples, determined by WAXD experiments during melting, are presented in Fig. 13. The stretched filled sample, which exhibited the best dynamic mechanical performance, also possessed the highest crystallinity index over the entire temperature range. On the other hand, the unfilled unstretched sample exhibited the poorest dynamic mechanical performance and also had the lowest value of X_C^T at all temperatures. The stretched unfilled sample exhibited a higher value of X_C^T at low temperatures in comparison with the unstretched filled sample, but this trend was reversed at higher temperatures. At 70 °C, the unstretched unfilled sample was totally molten, the stretched unfilled sample had $X_C^T = 0.8\%$, the unstretched filled sample had $X_C^T = 1\%$, and the stretched filled samples had $X_C^T = 2\%$. Therefore, we can conclude that the increase of crystallinity due to the presence of nanofillers is an important attribute to enhance the dynamic mechanical property, especially at the melting zone of the copolymer. Moreover, the observation that a detectable amount of crystals in the filled sample was stable at temperatures above the nominal melting temperature of the unfilled sample indicates that the effect of MCNFs on the polymer crystallization probably exceeds the typical role of a conventional nucleating agent. It implies the events of polymer chain adsorption on the nanofiller surface and the entropy restraints by the presence of MCNF become dominant, which is discussed below.

4. Discussion

4.1. Polymer chain dynamics in MCNF nanocomposites

Any reasonable comparison between the viscoelastic responses of the stretched and unstretched samples must take

into consideration the following observations: (1) the melting temperature of stretched polymer crystals ($T_{m,d}$) is higher than the melting temperature of the unstretched polymer crystals ($T_{m,u}$) according to the relation [52,53]

$$1/T_{m,d} = \left(1/T_{m,u}\right) - \left(\Delta S_{def}/\Delta H\right) \quad (2)$$

where ΔH is the heat of fusion that should be independent of deformation and ΔS_{def} is the difference of the entropy between the undeformed and the deformed states of the polymer crystals and (2) the absence of the γ phase in the stretched samples, in contrast to the unstretched sample. It is known that the thermal stability and the mechanical properties of the γ phase are lower than those of the α phase of iPP. Therefore, the differences in the dynamic mechanical spectra and the melting behavior between the filled and unfilled samples in their unstretched states cannot be directly attributed to the differences in the polymer chain dynamics. This is because (1) the content of the γ phase in the filled sample is lower than that in the unfilled sample and (2) the presence of MCNF may induce a certain degree of crystal orientation even in the unstretched samples. Both of these factors can contribute to the superior thermal stability and rheological performance of the unstretched filled sample.

On the other hand, the comparison between the filled and unfilled samples in their stretched states can be simplified because (1) the content of the γ phase in both samples is low (almost zero), such that the effect of the γ phase on the overall melting process can be neglected and (2) the orientation of the polymer crystals induced by mechanical stretching should far exceed the local orientation of chains in the vicinity of MCNF. In fact, the extent of crystal orientation and the amount of oriented crystals are the same (within the error of the measurement) for both filled and unfilled samples under stretched state at room temperature, whereas the superior thermal stability and enhanced rheological performance of the filled sample can be directly related to the interface between polymer chains and MCNF.

Fig. 14a illustrates the polymer crystal orientation fraction (i.e. the percentage of oriented crystals in the total crystalline phase) determined upon heating of the filled and unfilled samples in their stretched state. At room temperature, both samples exhibited the same amount of crystal orientation fraction. However, at high temperatures, the crystal orientation fraction was consistently higher in the unfilled sample than in the filled sample. Moreover, the integral breadth of the crystal peak corresponding to the hybrid α(110)/γ(111) reflection exhibited a lower value in the unfilled sample than in the filled sample (Fig. 14b). This observation indicates the existence of a notable amount of unoriented crystals in the filled sample at elevated temperatures. For the unfilled sample, upon gradual increase of temperature, some unoriented crystals were seen to melt first, followed by the melting of some oriented crystals, which can be explained by Eq. (2). The same trend was also seen in the filled sample, but in this case, surprisingly, a significant amount of unoriented crystals were stable at high temperatures.

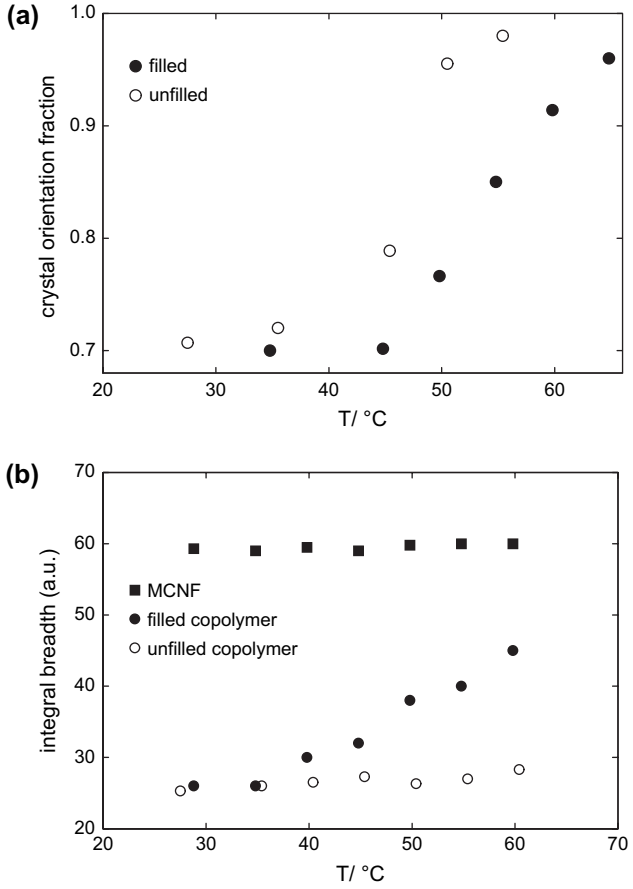

Fig. 14. Temperature dependence of (a) the oriented crystal fraction (filled circles for the filled sample, open circles for the unfilled sample) and (b) the integral breadths corresponding to the hybrid α(110)/γ(111) reflection of the polymer crystals (filled circles for the filled sample, open circles for the unfilled sample) and the (002) reflection of MCNF (squares). These values were determined during heating of the filled and unfilled samples in the stretched state.

The relationship between the oriented and unoriented crystalline fractions was displaced in favor of the unoriented crystalline fraction in the filled copolymer when compared to the unfilled one. Moreover, the mechanical spectra of the filled sample were significantly enhanced in the melting zone of the polymer. These effects are consistent with the hypothesis that the dynamics of polymer chains are retarded in the vicinity of the nanofiller (MCNF) interface. It is conceivable that at high temperatures, the mobility of the polymer chains remains restricted around the nanofiller interface, an effect that may favor the crystallization of the adsorbed chains into unoriented configurations. In this respect, the superior mechanical performance in the unstretched state can be correlated with the higher crystallinity in the filled sample. In addition, the total crystallinity of the stretched filled sample was found to be higher than that of the unstretched filled sample at elevated temperatures (Fig. 13), which is consistent with the mechanical spectra shown in Fig. 11.

In this study, we demonstrate that mechanical stretching is an effective means to fabricate a set of filled and unfilled samples with the same crystallinity, crystal phase and crystal

orientation. Such samples enabled the investigation of polymer chains surrounding the nanofillers in nanocomposites containing semicrystalline polymer matrix. It was found that the broadening of the high temperature side of the storage modulus peak took place, which has also been reported in a nanocomposite containing CNT dispersed in poly(vinyl alcohol) [54] (T_g region) as well as in other polymers filled with particles of high surface area [55]. Recent results from molecular dynamics simulations [56] indicated that the retardation of the polymer dynamics near the nanofiller interface can be attributed to the densification of the polymer chains in the adsorbed layer on the filler interface. Although the specific topography of a structured surface dictates the local configuration of polymer chains on the surface, the overall chain dynamics are governed by the polymer chains being trapped within the surface energy wells as well as the chain relaxation that occurs by migration of chains to the neighboring wells. Recently, a gradual change of the polymer dynamics approaching the nanofiller interface has been proposed [57] to rationalize the shift of the glass transition temperature (T_g) of the filled polymer. Taking into account the large surface area in MCNF, a significant portion of the polymer chain near the interface must exhibit the non-bulk characteristics, which would affect the overall viscoelastic response of the composite. In other words, the decreased chain mobility of the polymer chains near the MCNF interface is responsible for the broadening of the high temperature side of the storage modulus peak, which in turn contributes to the decrease of the tan δ value.

4.2. Tensile properties and MCNF orientation

It is clear that strong bonding between CNF and the polymer matrix is essential for the mechanical reinforcement of the polymer nanocomposite. For the semicrystalline polymer matrix, it has been argued that the presence of a crystalline polymer layer along the CNT can strongly enhance the load transfer [58]. Moreover, the presence of a crystalline shell around the MCNF could increase their effective aspect ratio and further enhance the reinforcement effect [59]. In the present study, our results indicated that at the same deformation a higher stress developed in the filled nanocomposites, but the amount of the strain-induced crystallinity and the degree of crystal orientation were lower in the composite than in pure sample (Fig. 9). This suggests that the polymer matrix experienced reduced stress as a result of the efficient load transfer to MCNFs. In this report, the role of nanofillers to the tensile properties was found to be more pronounced at elevated temperatures. There is experimental evidence [60], based on tensile data obtained below and above the T_g of two different matrices that this behavior reflects the increased mobility of the polymer chains, which suppress the motional restrictions of the nanoparticles. Within the melting zone of the polymer however, additional effects such as enhanced crystallinity (see above section) should also be considered.

The degree of nanofiller orientation is another critical parameter that dictates the tensile performance of the nanocomposite materials. This is seen in Fig. 7, where the tensile modulus and strength of the highly stretched filled copolymer are significantly higher than those of the stretched unfilled sample. Upon mechanical stretching, the degree of nanofiller orientation depends on the applied deformation and also on the developed stress (Fig. 6). Although the degree of MCNF orientation in the stretched sample is not so high, the partially oriented MCNF network could maintain its alignment upon melting of the polymer matrix (Fig. 14b). The four samples studied exhibited very different tensile properties (Fig. 7), but their storage modulus was quite close to each other (Fig. 11). This observation underlines the large difference in the mechanical performance of the materials, when examined under linear and non-linear viscoelastic conditions.

5. Conclusions

The mechanical performance of the MCNF-reinforced elastomeric EP copolymer is greatly affected by the degree of nanofiller orientation. By varying the stretching parameters (e.g. draw temperature and strain), a set of stretched filled/unfilled samples, containing similar crystallinity, crystal phase (α) and crystal orientation could be fabricated. These samples allowed the direct comparison of mechanical properties and chain dynamics between the filled and unfilled samples, thus revealing the effect of nanofiller on the semicrystalline polymer matrix. The mechanical spectra of the stretched filled samples showed pronounced broadening on the high temperature side of the storage modulus, which was also consistent with the increase in crystallinity. Results of this study indicated the reduced mobility of polymer chains in the vicinity of MCNF interface. The reduced mobility of the interface chains is responsible for the superior viscoelastic response of the nanocomposites; it is also responsible for the enhanced thermal stability of the oriented and unoriented polymer crystals.

Acknowledgements

The financial support of this work was provided by the Office of Naval Research (N000140310932), the National Science Foundation (DMR-0454887 and DMR-0405432) and the Department of Energy (DEFG0299ER45760) for the X27C beamline at NSLS, BNL. The authors also acknowledge the assistance of Dr. Lixia Rong for synchrotron experimental setup.

References

[1] Iijima S. Nature 1991;354:56.
[2] Qian D, Dickey EC, Andrews R, Rantell T. Appl Phys Lett 2000; 76:2868.
[3] Schadler LS, Giannaris SC, Ajayan PM. Appl Phys Lett 1998;73:3842.
[4] Biercuk MJ, Llaguno MC, Radosavljevic M, Hyun JK, Johnson AT, Fischer JE. Appl Phys Lett 2002;80:2767.
[5] Baughman RH, Zakhidov AA, de Heer WA. Science 2002;297:787.
[6] Li WZ, Xie SS, Qian LX, Chang BH, Zou BS, Zhou WY, et al. Science 1996;274:1701.

[7] Fan S, Chapline MG, Franklin NR, Tombler TW, Cassell AM, Dai H. Science 1999;283:512.
[8] Bower C, Zhu W, Jin S, Zhou O. Appl Phys Lett 2000;77:830.
[9] Kobacas C, Meitl MA, Gaur A, Shim M, Rogers JA. Nano Lett 2004;4:2421.
[10] Ko H, Peleshanko S, Tsukruk VV. J Phys Chem B 2004;108:4385.
[11] Xin H, Woolley AT. Nano Lett 2004;8:1481.
[12] Nagahara LA, Amlani I, Lewenstein J, Tsui RK. Appl Phys Lett 2004; 4:1481.
[13] Casavant MJ, Walters DA, Schmidt JJ, Smalley RE. J Appl Phys 2003;93:2153.
[14] Ajayan PM, Stephan O, Colliex C, Trauth D. Science 1994;265: 1212.
[15] de Heer WA, Chatelain A, Ugarte D. Science 1995;270:1179.
[16] Salalha W, Dror Y, Khalfin RL, Cohen Y, Yarin AL, Zussman E. Langmuir 2004;20:9852.
[17] Ran S, Burger C, Sics I, Yoon K, Fang D, Kim K, et al. Colloid Polym Sci 2004;282:802.
[18] Jin L, Bower C, Zhou O. Appl Phys Lett 1998;73:1197.
[19] Kim Y, Minami N, Kazaoui S. Appl Phys Lett 2005;86:073103.
[20] Hirsch A. Angew Chem Int Ed 2002;41:1853.
[21] Sun Y-P, Fu K, Lin Y, Huang W. Acc Chem Res 2002;35:1096.
[22] Niyogi S, Hamon MA, Hu H, Zhao B, Bhowmik P, Sen R, et al. Acc Chem Res 2002;35:1105.
[23] Blake R, Gunko YK, Coleman J, Cadek M, Fonseca A, Nagy JB, et al. J Am Chem Soc 2004;126:10226.
[24] Kelarakis A, Yoon K, Sics I, Somani R, Hsiao BS, Chu B. Polymer 2005;46:11591.
[25] Rodriguez NM. J Mater Res 1993;8:3233.
[26] Datta S, Srinivas S, Cheng CY, Tsou A, Lohse DJ. Rubber World 2003;229:55.
[27] Toki S, Sics I, Burger C, Fang D, Liu L, Hsiao BS, et al. Macromolecules 2006;39:3588.
[28] Frogley MD, Ravich D, Wagner HD. Comp Sci Technol 2003;63: 1647.
[29] Koerner H, Price G, Pearce NA, Alexander M, Vaia RH. Nat Mater 2004;3:115.
[30] Lozano K, Barrera EV. J Appl Polym Sci 2000;79:125.
[31] Kumar S, Doschi H, Srinivasarao M, Park JO, Schiraldi DA. Polymer 2002;43:1701.
[32] Finegan IC, Tibbetts GG, Glasgow DG, Ting J-M, Lake ML. J Mater Sci 2003;38:3485.
[33] Kelarakis A, Yoon K, Somani RH, Chen X, Hsiao BS, Chu B. Polymer 2005;46:11591.
[34] Kelarakis A, Yoon K, Sics I, Somani RH, Chen X, Hsiao BS, et al. J Macromol Sci Phys 2006;45:247.
[35] Fraser RDB, MacRae TP, Millar A, Rowlands RJ. J Appl Crystallogr 1976;9:81.
[36] Ran S, Zong X, Fang D, Hsiao B, Chu B, Ross R. J Appl Crystallogr 2000;33:1031.
[37] Nogales A, Hsiao BS, Somani RH, Tsou AH, Balta-Calleja FJ, Ezquerra TA. Polymer 2001;42:5247.
[38] Somani RH, Yang L, Hsiao BS, Agarwal PK, Fruitwala HA, Tsou AH. Macromolecules 2002;35:9096.
[39] Brucker S, Philips PJ, Mezghani K, Meille SV. Macromol Rapid Commun 1997;18:1.
[40] Perez E, Zucchi D, Sacchi MC, Forlini F, Bello A. Polymer 1999;40:675.
[41] Thomann R, Semke H, Maier R-D, Thomann Y, Scherble J, Mulhaupt R, et al. Polymer 2001;42:4597.
[42] Turner-Jones A. Polymer 1971;12:487.
[43] Feng Y, Jin X, Hay JN. J Appl Polym Sci 1998;68:381.
[44] Bhattacharyya AP, Sreekumar TV, Kumar S, Ericson LM, Hauge RH, Smalley RE. Polymer 2003;44:2373.
[45] Assouline E, Lustiger A, Barber AH, Cooper CA, Klein E, Wachtel E, et al. J Polym Sci Part B Polym Phys 2003;41:520.
[46] Valentini L, Biagiotti J, Kenny JM, Santucci S. Compos Sci Technol 2003;63:1149.
[47] Ge M, Sattler K. Science 1993;260:525.
[48] Zhou O, Fleming RM, Murphy DW, Chen CT, Haddon RC, Ramirez AP, et al. Science 1994;263:1744.
[49] Endo M, Takeuchi K, Hiraoka T, Furuta T, Kasai T, Sun X, et al. J Chem Solids 1997;58:1707.
[50] Auriemma F, De Rosa G, Boscato T, Corradini P. Macromolecules 2001;34:4815.
[51] De Rosa C, Auriemma F, Perretta C. Macromolecules 2004;37:6843.
[52] Yamamoto M, White JL. Polym Sci Part A-2 1971;9:1399.
[53] Tosaka M, Murakami S, Poompradub S, Kohjiya S, Ikeda Y, Toki S, et al. Macromolecules 2004;37:3299.
[54] Shaffer MS, Windle AH. Adv Mater 1991;11:937.
[55] Tsagaropoulos G, Eisenberg A. Macromolecules 1995;28:6067.
[56] Smith GD, Bedrov D, Borodin O. Phys Rev Lett 2003;90:226103.
[57] Starr WF, Schroder TB, Glotzer SC. Phys Rev E 2001;64:021802.
[58] Cadek M, Coleman JN, Barron V, Hedicke K, Blau W. J Appl Phys Lett 2002;81:5123–5.
[59] Coleman JN, Cadek M, Blake R, Nicolosi V, Ryan KP, Belton C, et al. Adv Funct Mater 2004;14:791.
[60] Shah D, Maiti P, Jiang DD, Batt CA, Giannelis EP. Adv Mater 2005;17:525.